PAAR-repeat proteins sharpen and diversify the Type VI secretion system spike

Published in final edited form as:
Nature. 2013 August 15; 500(7462): 350–353. doi:10.1038/nature12453.

PAAR-repeat proteins sharpen and diversify the Type VI secretion system spike

Mikhail M. Shneider[#1,2], **Sergey A. Buth**[#1], **Brian T. Ho**[3], **Marek Basler**[3], **John J. Mekalanos**[3,*], and **Petr G. Leiman**[1,*]

[1]École Polytechnique Fédérale de Lausanne (EPFL), BSP-415, 1015 Lausanne, Switzerland. [2]Shemyakin-Ovchinnikov Institute of Bioorganic Chemistry, Laboratory of Molecular Bioengineering, 16/10 Miklukho-Maklaya St., 117997 Moscow, Russia. [3]Department of Microbiology and Immunobiology, Harvard Medical School, 77 Avenue Louis Pasteur, Boston, MA 02115, USA.

[#] These authors contributed equally to this work.

Abstract

The bacterial type VI secretion system (T6SS) is a large multi-component, dynamic macromolecular machine that plays an important role in the ecology of many Gram negative bacteria. T6SS is responsible for translocation of a wide range of toxic effector molecules allowing predatory cells to kill both prokaryotic as well as eukaryotic prey cells[1-5]. The T6SS organelle is functionally analogous to contractile tails of bacteriophages and is thought to attack cells by initially penetrating them with a trimeric protein complex called the VgrG spike[6,7]. Neither the exact protein composition of the T6SS organelle nor the mechanisms of effector selection and delivery are known. Here we report that proteins from the PAAR (Proline-Alanine-Alanine-aRginine) repeat superfamily form a sharp conical extension on the VgrG spike, which is further involved in attaching effector domains to the spike. The crystal structures of two PAAR-repeat proteins bound to VgrG-like partners show that these proteins function to sharpen the tip of the VgrG spike. We demonstrate that PAAR proteins are essential for T6SS- mediated secretion and target cell killing by *Vibrio cholerae* and *Acinetobacter baylyi*. Our results suggest a new model of the T6SS organelle in which the VgrG-PAAR spike complex is decorated with multiple effectors that are delivered simultaneously into target cells in a single contraction-driven translocation event.

Correspondence and requests for materials should be addressed to P.G.L. (petr.leiman@epfl.ch) or J.J.M. (john_mekalanos@hms.harvard.edu). . [*]Correspondence to: john_mekalanos@hms.harvard.edu, petr.leiman@epfl.ch. .

Supplementary Information is available in the online version of the paper.

Author Contributions M.M.S. performed the initial bioinformatic analysis that led to the identification of PAAR proteins; M.M.S. cloned all VgrG and PAAR proteins for biochemical characterization and crystallization; M.M.S. and P.G.L. designed VgrG-PAAR binding experiments; M.M.S. and S.A.B. performed VgrG-PAAR binding experiments and purification of VgrG-PAAR complexes; S.A.B. crystallized VgrG-PAAR complexes and determined their crystal structures; J.J.M., M.B., and B.T.H. designed T6SS secretion and T6SS-mediated killing assay experiments involving PAAR mutants, B.T.H. and M.B. performed these experiments; B.T.H. performed the bioinformatics analysis of PAAR protein domain extensions. All authors participated in writing the manuscript.

Author Information The atomic coordinates and the structure factors of the refined atomic models of gp5-VCA0105 and gp5-c1882 complexes were deposited to the Protein Data Bank http://www.rcsb.org under the accession numbers 4JIV and 4JIW, respectively.

The authors declare no competing financial interests.

The T6SS organelle is a 1000 nm-long tubular structure consisting of an inner tube made of multiple copies of the Hcp protein and an external contractile sheath composed of VipA and VipB proteins (also called TssB/TssC in the literature)[3]. It has been visualized in two conformations (extended and contracted), which are both attached to the cell envelope by means of a baseplate complex[3]. Rapid contraction of the sheath results in translocation of the inner tube out of the predator cell and into the prey cell[3]. The trimeric VgrG spike protein is positioned at the end of the tube[7]. It is believed to penetrate the prey cell with its needle-shaped C-terminal β-helical domain. VgrG proteins can contain additional C-terminal domains that act as effectors[6] and may also bind effectors through undefined mechanisms[8].

Because VgrG proteins are orthologous to the central baseplate spikes of bacteriophages with contractile tails, we reasoned that additional structural components present in certain phage spikes might have corresponding orthologous components in T6SS. The cryoEM reconstruction of phage T4 baseplate shows that an unknown protein with a molecular weight between 7 and 23 kDa binds to the tip of the β-helical domain of the central spike protein gp5 [9]. We analyzed all known genes encoding small proteins in phage genomes with gp5-like spikes and compared them to T6SS genes. Proteins containing the PAAR-repeat motif were strongly represented in this group with gp5.4 being the corresponding protein of T4 phage. Furthermore, genes encoding proteins with PAAR motifs were frequently found immediately downstream from *vgrG*-like genes suggesting that the two are genetically linked[7]. Therefore, we devised a strategy to test the hypothesis that these PAAR proteins were binding to the tip of gp5 and VgrG proteins.

Careful examination of VgrG sequences showed that a β-structural repeat, which is presumed to be responsible for β-helix formation[6,10], either extends to the very C terminus of the protein or terminates with a glycine/serine-rich stretch (Extended Data Fig. 1). We surmised that the glycine/serine-rich stretch bends the polypeptide chain away from the β-helix without disturbing its tip, and that all VgrG β-helices have blunt ends resembling that of T4 gp5 β-helix. The X-ray crystal structure of one full-length VgrG trimer supports this conclusion (Sycheva LV, Shneider MM, Basler M, Ho B, Mekalanos JJ, Leiman PG. In preparation). Thus, we further hypothesized that the binding site for a PAAR protein was the blunt end of the β-helix and designed experiments to test this supposition.

Due to solubility problems of most tested VgrG and PAAR proteins, we used a soluble fragment of T4 gp5 β-helix (residues 484-575), which is known to fold into a stable native-like trimeric structure, as a platform for creating β-helices mimicking the blunt end of various VgrG spikes. We replaced the tip of gp5 β-helix (the last two β-strands) with an equivalent fragment from several putative β-helices of VgrGs from *Escherichia coli*, *Vibrio cholerae* and *Pseudomonas aeruginosa* (Extended Data Fig. 1). These gp5-VgrG chimeras were then co- expressed with various PAAR proteins in *cis* and in *trans* in different combinations (Extended Data Fig. 1). Surprisingly, the VCA0105 and c1882 PAAR proteins were found to bind not only to the ends of their endogenous VgrG proteins but also to the non-mutated wild type end of the gp5 β-helix as well.

The gp5-c1882 and gp5-VCA0105 complexes were purified to homogeneity and crystallized (Extended Data Table 1). The structures were solved by molecular replacement[11] using the corresponding gp5 β-helix fragment as a search model[10]. In both complexes, a single chain of the PAAR protein folds into a symmetrical cone-shaped structure with a sharp tip and a triangular base fully occupying the blunt end of the β-helix (Fig. 1). The cone contains 9 short β-strands, three of which create its base and participate in binding to gp5 and six others form three β-hairpins that point toward the vertex of the cone, but have different lengths. The PAAR proteins interact with the gp5 β-helix via a virtually flat hydrophobic patch and 14 or 16 hydrogen bonds for c1882 or VCA0105, respectively (Extended Data Fig. 2). In

both proteins, 12 hydrogen bonds between the main chain atoms of the tip of gp5 and those of the PAAR domain form a perfect triangle surrounding the central hydrophobic patch creating a unique binding platform (Extended Data Fig. 3). PISA software[12] shows that ~16.5% of the PAAR protein surface is buried in this interface and the free energy of interaction between the VgrG tip and c1882 or VCA0105 PAAR proteins is −5.5 kcal/mol or −3.4 kcal/mol, respectively.

The fold of the PAAR protein is stabilized by a Zn atom positioned close to the cone's vertex (Fig. 1d, Extended Data Fig. 4). The Zn binding site consists of three histidines and one cysteine - H14, H46, H54 and C81 in VCA0105 - that are very well conserved in close homologs (Extended Data Fig. 5a). These residues are replaced with similar or complementary metal-binding residues (arginines, lysines and glutamines) in more distant homologs suggesting that they also carry a metal ion roughly at the same position. The metal ion, being a natural ligand for this site, stabilizes the pointed tip of the PAAR domain and is likely to be important for its integrity during penetration of the target cell envelope.

The PAAR motif sequence is also conserved, albeit to a lower degree than the Zn binding site (Extended Data Fig. 5a). The PAAR motif functions to stabilize the fold by forming the central part of the structure where the three parts of the polypeptide chain meet and intertwine (Extended Data Fig. 5b, 5c). The three PAAR motifs interact with each other through the main chain hydrogen bonds that are shielded by hydrophobic residues from all sides (Fig. 1d). The distance between the C-alpha atoms of the third residue of the three PAAR motifs in both proteins is only 5.3±0.1 Å (Extended Data Fig. 5b, 5c). c1882 and VCA0105 show 61.3% sequence identity and as a consequence the two structures are very similar with a root mean square deviation (RMSD) of 0.53 Å between all the 94 C_α atoms comprising the backbone (Extended Data Fig. 6).

Given such a critical location of PAAR proteins within the T6SS organelle and their high structural conservation, we hypothesized that inactivation of *PAAR* genes would likely interfere with T6SS functions including protein secretion and prey cell killing. Because some $T6SS^+$ organisms have many gene products predicted to carry the PAAR motif, we focused on *Vibrio cholerae* strain 2740-80 and *Acinetobacter baylyi* ADP1, which each encode only two and three PAAR proteins, respectively. In *A. baylyi* inactivation of all three *PAAR* genes (*aciad0051*, *aciad0052*, *aciad2681*) led ~90% reduction in Hcp secretion (Extended Data Fig. 7) and at least a 10,000-fold decrease in T6SS-dependent killing of *E. coli* (Fig. 2a, 2c). Similarly, inactivation of both genes (*vca0105* and *vca0284*) that encode PAAR proteins in *V. cholerae* 2740-80 resulted in a ~100-fold decrease in T6SS-dependent killing of *E. coli* and ~70% reduction in Hcp secretion (Fig. 2b, 2c; Extended Data Fig. 7). Remarkably, in both bacterial species, mutants inactivated in single *PAAR* genes showed no or only a modest defect in the functionality of their T6SS apparatus (Fig 2) indicating that PAAR proteins within a species are interchangeable. We further attempted to complement these double and triple *PAAR* mutants with heterologous *PAAR* genes but these experiments were inconclusive (Extended Data Fig. 8). Thus, PAAR proteins may be very specific for their cognate VgrG proteins in the context of the functional T6SS organelle.

The dramatic reduction in Hcp secretion in the triple *PAAR* gene knockout mutant of *A. baylyi* suggests that PAAR proteins participate in the assembly of the T6SS complex by either nucleating the folding of VgrG trimers or regulating their incorporation into the T6SS organelle. Similar to the T4 phage system in which mutants lacking gp5 (VgrG ortholog) are tailless[13], any disruption in VgrG trimeric assembly will likely block the assembly of the T6SS organelle. Alternatively, PAAR proteins may be important for another function of the apparatus such as translocation of the VgrG spike through the predator outer membrane during a sheath contraction event.

The PAAR-repeat proteins form a diverse superfamily called CL15808 in the CDD database[14] that contains three families PF05488, COG4104, and PF13665 (or DUF4150). The first two families are similar and describe PAAR domains that are on average ~95 residues long whereas the PF13665 family is somewhat more distant and its typical members contain ~130 amino acids. The crystal structures reported here include representatives of the PF05488 family. Hundreds of hypothetical proteins in the database contain PAAR domains that are extended both N- and C-terminally by domains with various predicted functions (Extended Data Fig. 9). The crystal structure shows that the termini of the PAAR domain are open to solution and thus can be extended without distorting the VgrG binding site (Fig. 1, Extended Data Fig. 6).

The C-terminal domains of many hypothetical PAAR proteins are predicted to have various enzymatic activities that are toxic for prokaryotic and eukaryotic cells (Extended Data Fig. 9). Very similar putative effector domains can be found fused to the C-termini of VgrG proteins (e.g., VIP2 ADP-ribosyl transferase). Binding of these larger PAAR proteins to the tip of VgrG spikes would decorate the T6SS spike with a great variety of effector domains. To test this hypothesis, we expressed a vsvG epitope-tagged version of the ACIAD2681 PAAR protein in the WT *A. baylyi* ADP1 and in its triple *PAAR* gene knockout mutant (Fig. 3). The epitope-tagged protein was secreted by T6SS and fully restored T6SS-mediated killing of *E. coli* in the triple *PAAR* gene knockout strain (Fig. 2a, 3), suggesting that other effector proteins fused to PAAR domains will likely also be targeted for secretion by binding the tip of VgrG trimers.

VCA0284, the larger of the two *V. cholerae* V52 PAAR proteins, carries a transthyretin domain (TTR) at its C terminus, which is a very common architecture of PAAR proteins (Extended Data Fig. 9). TTR is an immunoglobulin-like domain that is known to form oligomeric structures in which these domains interact with each other or with other partners[15]. Thus, PAAR-associated TTR domains may act as adapters to further decorate the VgrG tip with effectors displaying TTR domains or serve to bind the spike to other TTR domain-containing proteins such as the TssJ/SciN lipoprotein[16], an outer membrane structural component of the T6SS “baseplate”[3].

Besides being in T6SS gene clusters, many *PAAR* genes are frequently found downstream of *vgrG* genes[6], which in turn, are often encoded by Rhs elements (accessory sequences that have the hallmarks of horizontally acquired DNA, Extended Data Fig. 9). A recent report[17] shows that two different nucleases encoded by the *rhsA* and *rhsB* genes of *Dickeya dadantii* are delivered into target cells in a VgrG-dependent process, suggesting that the T6SS locus of this organism mediates translocation of these effectors. Interestingly, both RhsA and RhsB proteins contain PAAR repeat regions and other features that categorize them as Class 7 PAAR domain architecture proteins (Extended Data Fig. 9b). Thus, our working model (Fig. 4) predicts that these T6SS nuclease effectors should bind to the tip of VgrG trimers through their PAAR repeat domains and in this way be targeted for secretion and translocation into prey cells.

The structural, functional, and bioinformatic findings summarized above allow us to make several conclusions and predictions. Because a PAAR-repeat protein caps the end of the β-helix of a VgrG spike, it is in fact the piercing tip that is responsible for the initial event of creating an opening in the target cell envelope. Furthermore, because the crystal structure demonstrates that the canonical PAAR-repeat domain can be extended N- or C-terminally without distorting its structure or its VgrG β-helix binding site, we predict that large PAAR proteins carrying effector domains will likely also bind to VgrG spikes and be translocated into target cells by the T6SS organelle. Considering the findings reported here and other published data we propose that there are five mechanisms by which effectors can be

incorporated into the T6SS spike complex (Fig. 4). Three of them – 1) C-terminal extensions of the VgrG spike[6], 2) Binding surface features on the VgrG protein[8,18], and 3) N- or C-terminal extensions of the PAAR protein[17] – have direct or indirect experimental evidence. Two others – 4) Binding surface features or additional domains (e.g., the TTR domain) on PAAR proteins and 5) Incorporation into the cavity formed by the gp27 domain of VgrG – remain speculative. Thus, the T6SS machine may be capable of delivering a multifunctional 'cargo' – or **M**ultiple **E**ffector T**R**anslocation **V**grG (**MERV**) spike – into the target prey cell in a single molecular translocation event driven by T6SS sheath contraction.

Methods

Cloning and protein expression

The gp5 fragment containing residues 484-575 was cloned into the in-house designed expression vector pEEva2 with the help of the In-Fusion system (Clontech). The pEEva2 vector is a derivative of the pET-23a expression plasmid (Novagen) with a modified multiple cloning region. The T7-tag was replaced with a $MGSSH_6SSG$ polyhistidine tag (His-tag) followed by a sequence containing a tobacco etch virus (TEV) protease cleavage site (ENLYFQ^GSGS). Upon expression and after TEV cleavage, the gp5 fragment contained four residues (GSGS) upstream of residue 484. The C-terminal residues of gp5 were modified by performing PCR with long primers containing the required mutations (Extended Data Fig. 1).

For expression in *cis*, *PAAR* genes were cloned downstream from the gp5 fragment. The spacer between the stop codon of gene *5* and the first codon of *PAAR* genes contained a standard ribosome binding sequence and was about 15 bases long.

For expression in *trans*, *PAAR* genes were cloned into the pATE vector (chloramphenicol selection), which is a modified version of the pACYCDuet-1 expression plasmid (Novagen). The dual cloning site of the pACYCDuet-1 vector was replaced by the multiple cloning site from the pEEva2 vector. The cloned PAAR proteins retained their wild type N and C termini (i.e. were tag-free).

Expression and purification of gp5-PAAR complexes

Gp5-PAAR complexes were expressed in *Escherichia coli* B834(DE3) cells grown in the 2×TY medium containing ampicillin at 100 μg/ml for the *cis* constructs and, additionally, chloramphenicol at 34 μg/ml for the *trans* constructs. The cultures with a total volume of 2 liters were incubated at 37° C with shaking at 200 rpm until the culture reached the optical density (OD) of 0.6 (600 nm wavelength). The culture was cooled down to 18°C, and the protein expression was induced by an addition of isopropyl-β-D-thiogalactoside to a final concentration of 1 mM. The expression continued overnight.

The cells were harvested on the following day by centrifugation at 8000 g at 4°C for 10 min. The cell pellet was resuspended in a lysis buffer that contained 50 mM TrisCl pH 8.0, 300 mM NaCl, 5 mM Imidazole. The cells were lysed by ultrasonication, which was performed on ice with the temperature of the lysate maintained below 10° C. The lysate was then centrifuged at 25000 g, 4°C for 10 min. The supernatant was applied to a Ni column (5ml GE HisTrap FF Crude). The non-specifically bound material was removed by washing the columns with 10 column volumes of a washing buffer (50 mM TrisCl pH 8.0, 300 mM NaCl, 20 mM Imidazole. The affinity bound material was eluted with 10 column volumes of an elution buffer (20mM TrisCl pH 8.0, 300mM NaCl, 250mM Imidazole).

The fractions containing the target protein were pulled together and the TEV protease was added to have a concentration of 10% (w/w) of the target protein. The mixture was then

placed into a dialysis bag, and the proteolysis continued overnight with a simultaneous dialysis against a buffer optimal for TEV cleavage (10mM TrisCl pH 8.0, 3mM DTT, 1.5mM EDTA). The digested protein was further purified by ion-exchange chromatography performed with a GE Mono Q 10/100 GL column connected to an AKTApurifier 100 system (GE Healthcare Life Sciences). The sample was loaded onto the column that was equilibrated with buffer A (20mM TrisCl pH 8.0) and eluted with a linear gradient against buffer B (20mM TrisCl pH 8.0, 1M NaCl). The gradient extended from 0% to 65% of the buffer B concentration. Relevant fraction were combined and concentrated using Sartorius ultrafiltration devices with a molecular weight cutoff of 10,000 to a volume of ~5ml. This sample was then loaded onto a GE HiLoad 16/60 Superdex 200 size-exclusion column pre-equilibrated with 10mM TrisCl pH 8.0, 150mM NaCl. The fractions containing pure gp5G484-PAAR complexes were combined and concentrated to 25 mg/ml with the help of a similar Sartorius ultrafiltration devices and without changing the buffer. The protein was stored in the same buffer at +4°C until it was used for crystallization. All purification buffers and the final protein solution contained NaN_3 at a concentration of 0.02% (w/v).

Identification of gp5-PAAR complexes

The purification procedure employed metal affinity chromatography based on the N-terminal His-tags of gp5 fragments with slightly modified C-termini (Extended Data Fig. 1), and thus led to accumulation of two protein species - gp5-PAAR complexes and gp5 fragments alone. The β-helical fragment of gp5 used in this study does not fully denature in sodium dodecyl sulfate polyacrylamide gel (SDS-PAGE), and runs as several species with apparent molecular weights (MW) of 10-30 kDa. Most of the PAAR proteins (MW ~9.7 kDa) had the same SDS-PAGE mobility as the fastest migrating band of gp5 fragments (MW ~10 kDa). However, these species were easily separable by a combination of high resolution anion exchange and analytical size exclusion chromatographies (monoQ and Superdex 75 resins, respectively). The gp5 fragment is a highly negatively charged β-helix[10] that binds to the monoQ anion exchange resin strongly. Consequently, gp5 fragments that were free from PAAR proteins eluted from the monoQ resin by a buffer with a specific conductivity of 24-29 mS/cm. All gp5-PAAR complexes discussed in this paper were found to be much weaker anionic binders and eluted from the monoQ resin by a buffer with a specific conductivity of 18-25 mS/cm. Furthermore, size exclusion profiles (Superdex 75 10/300 GL) of all gp5- PAAR complexes had only one peak centered at 10.34±0.06 ml, whereas gp5 fragments free from PAAR proteins formed various oligomers and eluted at different positions of the chromatogram. The VCA0284 PAAR protein containing the transthyretin domain was prone to aggregation and the gp5-VCA0284 complex was unsuitable for size-exclusion chromatography. Expression of VCA0284 in the presence of the gp5_VCA0018 or gp5_VCA0123 chimeras led to an almost complete loss of gp5 from solution indicating complex formation.

Crystallization and structure determination of gp5-PAAR complexes

The initial crystallization screening was carried out by the sitting drop method in 96 well SWISSCI 2-lens MRC plates using Jena Bioscience crystallization screens. Bio-Tek Precision XS and TTP Labtech mosquito pipetting robots were employed for preparing crystallization plates and setting up drops each containing 200 nl of the protein and the same volume of the well solution. Optimization of crystallization conditions was performed in 24 well SuperClear plates and thick siliconized cover slides (both from Jena Bioscience) by hanging drop vapor diffusion. Crystallization drops of the 24-well plate setup contained 1.25 μl of the protein solution in 10 mM TrisCl pH 8.0, 150 mM NaCl mixed with an equal volume of the well solution. Best crystals of the gp5-c1882 complex were obtained with the protein having the initial concentration of 13.5 mg/ml and equilibrated against 500 μl of the well solution containing 100-150 mM $CaCl_2$, 13-15% PEG 3350, 100 mM MES pH 6.5.

Best crystals of the gp5-VCA0105 complex were obtained with the protein at 15 mg/ml and equilibrated against 500μl of the well solution containing 13-14% PEG 2000, 100 mM NaAc pH 5.0.

For data collection, the crystals were dipped for 20-45 seconds into cryo solutions containing either 30% of glycerol for gp5-c1882 or 25% of 2-methyl-2,4-pentanediol for gp5- VCA0105 in addition to the well solution components and flash frozen in a vaporized nitrogen stream at 100 K. Collection of diffraction data and fluorescent scans was carried out at the PXI and PXIII beam lines of the Swiss Light Source (SLS) at the Paul Scherrer Institute (Villigen, Switzerland), respectively, using X-rays with a wavelength of 1.000 Å for both crystals. Best gp5-c1882 and gp5-VCA0105 crystals diffracted to 3.4 Å and 1.9 Å resolution limits, respectively. The diffraction data was indexed, integrated, and scaled with XDS[27] (Extended Data Table 1). The structure of the gp5-c1882 complex was solved by molecular replacement with PHASER[19] using a fragment of the gp5-gp27 complex crystal structure containing residues 484-575 of gp5 (PDB ID 1K28) as a search model[10]. As the asymmetric unit contained four gp5-c1882 complexes, non-crystallographic symmetry (NCS) averaging was used to improve the electron density prior to model building. The model was built manually with COOT[28] and refined with REFMAC5[21] and PHENIX[20] using NCS for torsion angles restraints. The structure of gp5-c1882 was subsequently used as a search model to solve the structure of the gp5-VCA0105 complex by molecular replacement with PHASER[19]. There was only one complex per asymmetric units. The structure was refined with PHENIX[20] and COOT[28].

Both refined structures, gp5-VCA0105 and gp5-c1882, had excellent stereochemical parameters (see also Extended Data Table 1). All main chain dihedral angles of the gp5-VCA0105 structure were found in the most favored regions of the Ramachandran plot. The gp5-c1882 structure had 97.3 % of its main chain dihedral angles in the most favored regions of the Ramachandran plot, 2.7% in the additionally allowed regions, and none in the disallowed region.

Bioinformatics

Putative orthologs of PAAR repeat proteins were identified with the help of HMMER[23]. A search for high confidence hits to PFAM[29] domains PF05488 or PF13665 that describe the two distinct PAAR repeat domains resulted in 1353 PAAR domain-containing proteins. Phage proteins and orphan genes were excluded from this analysis. Functional assignment of extension domains was based on high confidence hits obtained with the help HHpred[24], HMMER[23], CDD[14], and CDART[25] web services.

Bacterial killing assays

Overnight cultures of *V. cholerae* 2740-80, *A. baylyi* ADP1 and *E. coli* MG1655 were washed in LB and diluted 50-200× into fresh LB and cultivated for 2.5–3.5 hr to reach the OD of ~0.5–1.0. Cells were pelleted by centrifugation at 4,000×g for 5 minutes and mixed at OD ~10 in 1:1 ratio. After 2 hr at 37 C, bacterial spots were cut out and the cells were resuspended in 1 ml LB. The cellular suspension was serially diluted in LB, and 5 μl of the suspensions was spotted on selective plates (streptomycin for *V. cholerae* and *A. baylyi*, and gentamicin for *E. coli*). *aciad2681* was expressed basally from the plasmid pMMB67EH [26]. PAAR protein complementation in *V. cholerae* was done by cloning the indicated *PAAR* genes into pBAD24 [30] and inducing with the appropriate concentrations of L-arabinose. Two- tailed Student's *t*-test was used to interpret the statistical significance of the number of the colony forming units.

Protein secretion

Overnight cultures of *V. cholerae* 2740-80 and *A. baylyi* ADP1 were washed in LB and diluted 200× into fresh LB and cultivated for 5 hr at 37 C. 1 mL of culture supernatants were passed through 0.2 μM filter, precipitated with TCA, subjected to 12% SDS-PAGE and stained with Coomassie Blue. The recombinantly expressed ACIAD2681 PAAR protein carried a C-terminal vsvG epitope tag (YTDIEMNRLGK). Western blots were performed on the TCA precipitated samples following standard methodology using anti-vsvG primary antibodies (Sigma). Band intensities were quantified using the Fiji software[31].

Molecular graphics

UCSF Chimera[32] was used to prepare Figure 1 and Extended Data Figures 2-6.

Supplementary Material

Refer to Web version on PubMed Central for supplementary material.

Acknowledgments

We thank the entire staff of the Swiss Light Source PX beamlines and Dr. Vincent Olieric in particular for support related to crystallographic data collection. The project was made possible by the Swiss National Science Foundation (grant 31003A_127092) and EPFL funding to P.G.L., and grants AI-026289 and AI-01845 from the NIAID to J.J.M.

References

1. Pukatzki S, et al. Identification of a conserved bacterial protein secretion system in Vibrio cholerae using the Dictyostelium host model system. Proc Natl Acad Sci U S A. 2006; 103:1528–33. [PubMed: 16432199]
2. Mougous JD, et al. A virulence locus of Pseudomonas aeruginosa encodes a protein secretion apparatus. Science. 2006; 312:1526–30. [PubMed: 16763151]
3. Basler M, Pilhofer M, Henderson GP, Jensen GJ, Mekalanos JJ. Type VI secretion requires a dynamic contractile phage tail-like structure. Nature. 2012; 483:182–6. [PubMed: 22367545]
4. Kapitein N, Mogk A. Deadly syringes: type VI secretion system activities in pathogenicity and interbacterial competition. Curr Opin Microbiol. 2013
5. Basler M, Ho BT, Mekalanos JJ. Tit-for-Tat: Type VI Secretion System Counterattack during Bacterial Cell-Cell Interactions. Cell. 2013; 152:884–94. [PubMed: 23415234]
6. Pukatzki S, Ma AT, Revel AT, Sturtevant D, Mekalanos JJ. Type VI secretion system translocates a phage tail spike-like protein into target cells where it cross-links actin. Proc Natl Acad Sci U S A. 2007; 104:15508–13. [PubMed: 17873062]
7. Leiman PG, et al. Type VI secretion apparatus and phage tail-associated protein complexes share a common evolutionary origin. Proc Natl Acad Sci U S A. 2009; 106:4154–9. [PubMed: 19251641]
8. Dong TG, Ho BT, Yoder-Himes DR, Mekalanos JJ. Identification of T6SS-dependent effector and immunity proteins by Tn-seq in Vibrio cholerae. Proc Natl Acad Sci U S A. 2013; 110:2623–8. [PubMed: 23362380]
9. Kostyuchenko VA, et al. Three-dimensional structure of bacteriophage T4 baseplate. Nat Struct Biol. 2003; 10:688–93. [PubMed: 12923574]
10. Kanamaru S, et al. Structure of the cell-puncturing device of bacteriophage T4. Nature. 2002; 415:553–557. [PubMed: 11823865]
11. Rossmann MG, Blow DM. The detection of sub-units within the crystallographic asymmetric unit. Acta Crystallographica. 1962; 15:24–31.
12. Krissinel E, Henrick K. Inference of macromolecular assemblies from crystalline state. J Mol Biol. 2007; 372:774–97. [PubMed: 17681537]

13. Kikuchi Y, King J. Genetic control of bacteriophage T4 baseplate morphogenesis. II. Mutants unable to form the central part of the baseplate. J Mol Biol. 1975; 99:673–694. [PubMed: 765482]
14. Marchler-Bauer A, et al. CDD: conserved domains and protein three-dimensional structure. Nucleic Acids Res. 2013; 41:D348–52. [PubMed: 23197659]
15. Hamburger ZA, Brown MS, Isberg RR, Bjorkman PJ. Crystal structure of invasin: a bacterial integrin-binding protein. Science. 1999; 286:291–5. [PubMed: 10514372]
16. Felisberto-Rodrigues C, et al. Towards a structural comprehension of bacterial type VI secretion systems: characterization of the TssJ-TssM complex of an Escherichia coli pathovar. PLoS Pathog. 2011; 7:e1002386. [PubMed: 22102820]
17. Koskiniemi S, et al. Rhs proteins from diverse bacteria mediate intercellular competition. Proc Natl Acad Sci U S A. 2013; 110:7032–7. [PubMed: 23572593]
18. Hachani A, et al. Type VI secretion system in Pseudomonas aeruginosa: secretion and multimerization of VgrG proteins. J Biol Chem. 2011; 286:12317–27. [PubMed: 21325275]
19. McCoy AJ, et al. Phaser crystallographic software. Journal of applied crystallography. 2007; 40:658–674. [PubMed: 19461840]
20. Adams PD, et al. The Phenix software for automated determination of macromolecular structures. Methods. 2011; 55:94–106. [PubMed: 21821126]
21. Murshudov GN, et al. REFMAC5 for the refinement of macromolecular crystal structures. Acta Crystallogr D Biol Crystallogr. 2011; 67:355–67. [PubMed: 21460454]
22. Emsley P, Lohkamp B, Scott WG, Cowtan K. Features and development of Coot. Acta Crystallogr D Biol Crystallogr. 2010; 66:486–501. [PubMed: 20383002]
23. Finn RD, Clements J, Eddy SR. HMMER web server: interactive sequence similarity searching. Nucleic Acids Res. 2011; 39:W29–37. [PubMed: 21593126]
24. Soding J, Biegert A, Lupas AN. The HHpred interactive server for protein homology detection and structure prediction. Nucleic acids research. 2005; 33:W244–8. [PubMed: 15980461]
25. Geer LY, Domrachev M, Lipman DJ, Bryant SH. CDART: protein homology by domain architecture. Genome research. 2002; 12:1619–23. [PubMed: 12368255]
26. Furste JP, et al. Molecular-Cloning of the Plasmid Rp4 Primase Region in a Multi-Host-Range Tacp Expression Vector. Gene. 1986; 48:119–131. [PubMed: 3549457]
27. Kabsch W. XDS. Acta crystallographica. Section D, Biological crystallography. 2010; 66:125–32.
28. Emsley P, Cowtan K. Coot: model-building tools for molecular graphics. Acta Crystallogr D Biol Crystallogr. 2004; 60:2126–32. [PubMed: 15572765]
29. Finn RD, et al. The Pfam protein families database. Nucleic acids research. 2010; 38:D211–22. [PubMed: 19920124]
30. Guzman LM, Belin D, Carson MJ, Beckwith J. Tight regulation, modulation, and high-level expression by vectors containing the arabinose PBAD promoter. J Bacteriol. 1995; 177:4121–30. [PubMed: 7608087]
31. Schindelin J, et al. Fiji: an open-source platform for biological-image analysis. Nat Methods. 2012; 9:676–82. [PubMed: 22743772]
32. Pettersen EF, et al. UCSF Chimera--a visualization system for exploratory research and analysis. Journal of computational chemistry. 2004; 25:1605–12. [PubMed: 15264254]
33. Kyte J, Doolittle RF. A simple method for displaying the hydropathic character of a protein. J Mol Biol. 1982; 157:105–32. [PubMed: 7108955]
34. Bearden JA. X-Ray Wavelengths. Reviews of Modern Physics. 1967; 39:78. &.
35. Crooks GE, Hon G, Chandonia JM, Brenner SE. WebLogo: a sequence logo generator. Genome research. 2004; 14:1188–90. [PubMed: 15173120]
36. Altschul SF, Gish W, Miller W, Myers EW, Lipman DJ. Basic local alignment search tool. J Mol Biol. 1990; 215:403–410. [PubMed: 2231712]

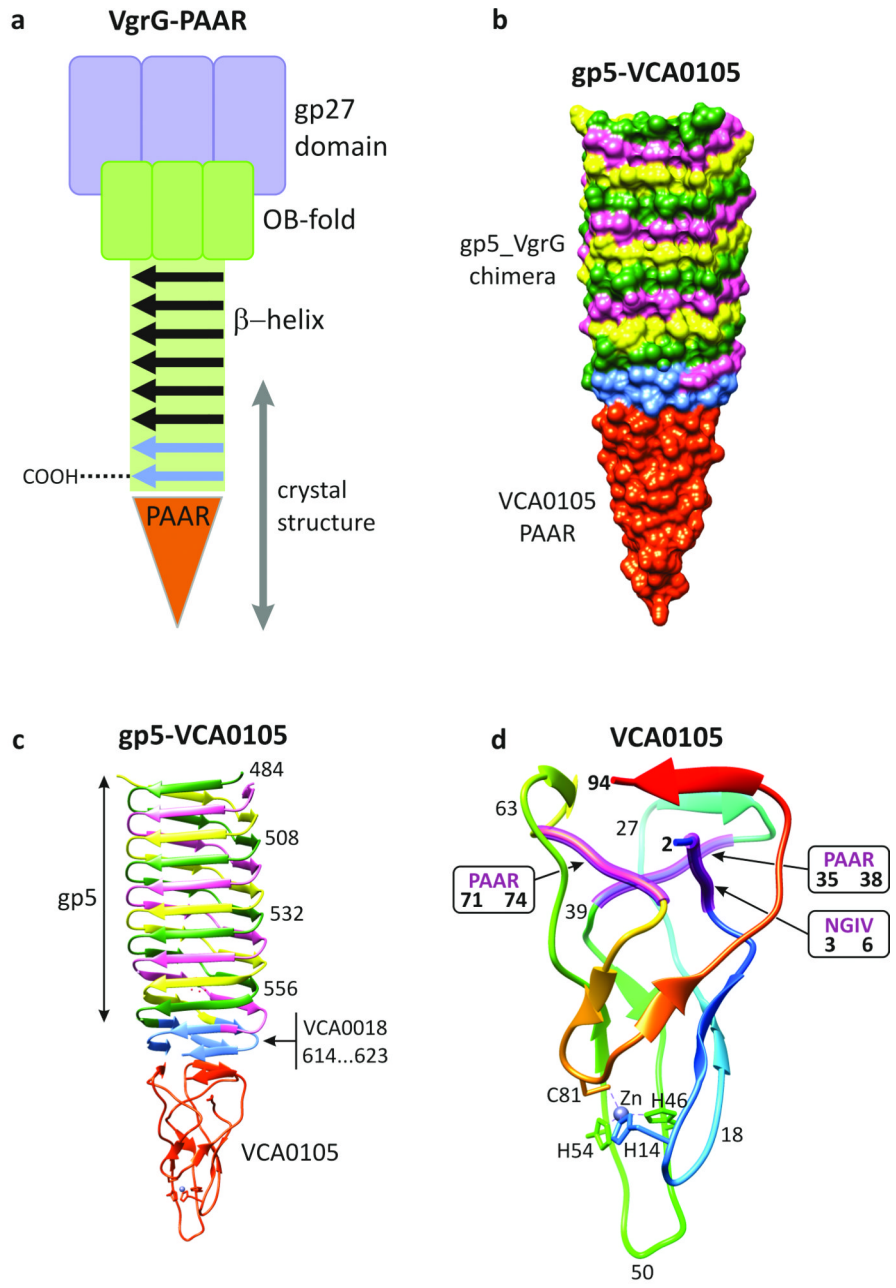

Figure 1.

Crystal structure of the VCA0105 PAAR-repeat protein bound to its VgrG-like partner. **a**, Schematic representation of the conserved domains comprising the VgrG-PAAR complex. The last strands of the β-helix that form the PAAR binding site are in light blue. Gray arrow shows the fragment roughly corresponding to the crystal structure. **b**, Molecular surface representation of the gp5_VCA0018-VCA0105 complex crystal structure. Each protein chain is labeled with its own color. **c**, Ribbon diagram of the gp5_VCA0018- VCA0105 complex. **d**, The polypeptide chain of the VCA0105 PAAR protein is colored in rainbow colors with N terminus in blue and C terminus in red. Residues responsible for Zn binding are labeled.

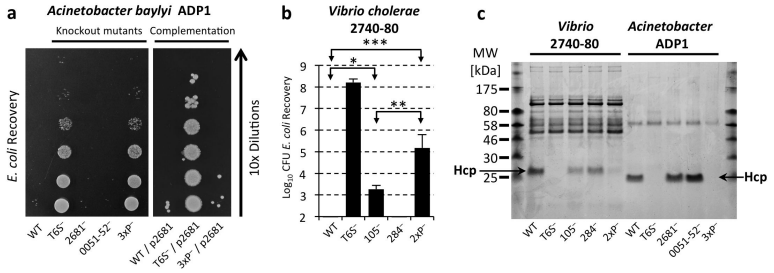

Figure 2.

PAAR proteins are required for full functionality of the T6SS in *Vibrio cholerae* and *Acinetobacter baylyi*. **a**, Recovery of viable *E. coli* MG1655 after co-incubation with *A. baylyi* ADP1 (WT) and its T6SS and *PAAR* genes knockout mutants. The following genes were inactivated in the mutants shown: T6S$^-$ – *aciad2688* to *aciad2694*; 2681$^-$ – *aciad2681*; 0051-52$^-$ – both *aciad0051* and *aciad0052*; 3×P$^-$ – all three *PAAR* genes *aciad0051*, *aciad0052* and *aciad2681*. *Right subpanel*: Leaky, basal expression of the *aciad2681 PAAR* gene from plasmid pMMB67EH[26], labeled as p2681, restores the killing defect in the triple *PAAR* mutant. **b**, Recovery of *E. coli* MG1655 colony forming units after co-incubation with *V. cholerae* 2740-80 and its T6SS and *PAAR* genes knockout mutants, which are labeled as follows: T6S$^-$ – *vipA*; 10S$^-$ – *vca0105*; 284$^-$ – *vca0284*; 2×P$^-$ – *vca0105* and *vca0284*. Symbols *, **, and *** indicate deviations from the WT with p-values of 6×10^{-3}, 8×10^{-3}, and 5×10^{-7}, respectively, for a sample size of 8. Error bars represent one standard deviation. **c**, SDS-PAGE assay for T6SS-dependent secretion of Hcp proteins by the parental strains and T6SS and *PAAR* genes knockout mutants. Panels **a** and **c** show one out of three experiments with similar outcomes.

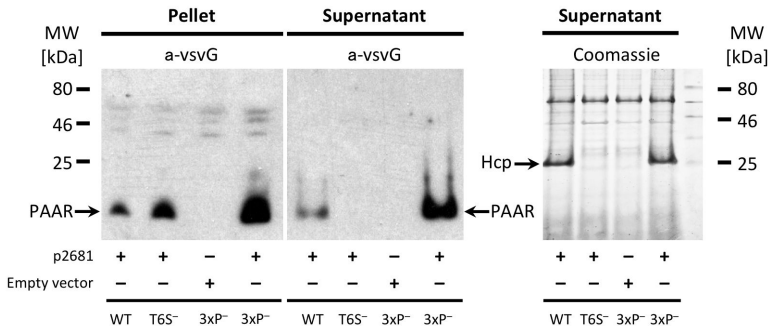

Figure 3.

The vsvG epitope-tagged PAAR protein ACIAD2681 is secreted by *A. baylyi* ADP1. *Left panels:* T6SS-dependent secretion of vsvG epitope-tagged ACIAD2681 expressed from plasmid pMMB67EH. *Right panel*: vsvG epitope-tagged ACIAD2681 fully restores the Hcp secretion defect of the triple knockout *PAAR* mutant of *A. baylyi* ADP1. The mutants are labeled as in Fig. 2. A representative of three identical experiments was chosen for each panel.

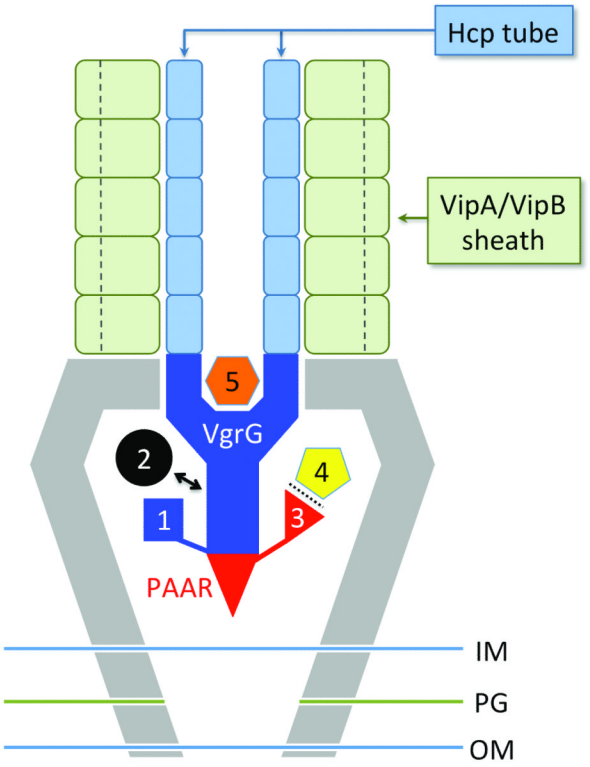

Figure 4.

Multiple **E**ffector T**R**anslocation **V**grG (**MERV**) model for the organization of the T6SS central spike/baseplate. Effectors are predicted to be loaded onto the spike complex by five distinct mechanisms: 1) C-terminal extensions of the VgrG spike; 2) Non-covalent binding to the VgrG spike; 3) N- or C-terminal extensions of the PAAR protein; 4) Non- covalent binding to the PAAR protein or its extension domains; 5) Incorporation into the cavity formed by the gp27 domain of VgrG. A single T6SS sheath contraction event translocates the VgrG spike with all of its cargo proteins into a nearby target cell. Other proteins making up the T6SS “baseplate” are not labeled but presumably reside within or attached to the inner and outer membranes and peptidoglycan layer (IM, OM, and PG, respectively).